



Characterization of ceramic tiles prepared from two clays from Sergipe — Brazil

A.C.S. Alcântara ^a, M.S.S. Beltrão ^a, H.A. Oliveira ^b, I.F. Gimenez ^a, L.S. Barreto ^{a,*}

^a *Laboratório de Tecnologia de Materiais, Universidade Federal de Sergipe-UFS,*

Av. Marechal Rondon s/n, São Cristóvão-SE-49100-000, Brazil

^b *Cerâmica Santa Márcia - Aracaju-SE, Brazil*

Received 16 March 2007; received in revised form 2 May 2007; accepted 10 May 2007

Abstract

We report an investigation of stain formation after use of clay–ceramic floor tiles produced by an industry from Sergipe, Brazil. Two types of raw materials have been used (C1 and C2) and test specimens were prepared at firing temperatures of 1000, 1120 and 1140 °C, being afterwards immersed in muriatic acid, evidencing stain formation for C1 tiles. After ICP chemical analysis, the original clays and tiles were characterized by powder X-ray diffraction (XRD) and TGA measurements, evidencing that C1 contained a higher carbonate percent than C2. Tile specimens were evaluated by X-ray diffraction (XRD), scanning electron microscopy (SEM), flexural strength, apparent density, linear shrinkage, and water absorption. In contrast to tiles prepared from C2, those prepared from C1 presented higher interparticle porosity and both linear shrinkages and water absorption variations with temperature were very incipient, suggesting that the high porosity and the low sintering caused the low staining resistance.

© 2007 Elsevier B.V. All rights reserved.

Keywords: Ceramic floor tiles; Color inhomogeneity; Staining resistance; Clays

1. Introduction

Ceramic tiles are materials of variable porosity, composed essentially of clays and other inorganic raw materials such as quartz, iron oxides and carbonates (Sánchez-Muñoz et al., 2002a; Monteiro and Vieira, 2004). In the fabrication process, the raw materials are mixed in proportions taking into account the influence of each component in the properties of the final materials, followed by general processing steps such as pressing and firing (Sousa and Holanda, 2005). Common components that play fundamental roles for optimum processing, and hence

performance of the final products, are kaolin or kaolinitic clay for plasticity, feldspar for fluxing and silica as filler material (Kamseu et al., 2007). In the processing steps, sintering of the ceramic mass is fundamental to adjust several desired properties and occurs in general through liquid-phase formation, thus the presence of components such as low-melting clays is very important (Sánchez-Muñoz et al., 2002b). In general, ceramic tiles must present good resistance to formation of stains and scratches, which are normally related to the porosity as well as low mechanical properties. High porosity is an undesired feature in the final product and its occurrence is related to inappropriate sintering conditions such as inadequate firing temperature as well as to the imbalance of components in the mass composition (Sánchez-Muñoz et al., 2002a).

* Corresponding author. Tel.: +55 79 2105 6652; fax: +55 79 2105 6651.
E-mail address: ledjane@ufs.br (L.S. Barreto).

Stain formation has been observed after installation of some floor tiles from a local ceramic industry, which uses natural clays from Sergipe State, Brazil. Previous works report that problems of low staining resistance may be related to exposure of the intraparticle porosity upon polishing, in special considering external sources of inhomogeneities (Arantes et al., 2001; Sanchez et al., 2006; Cavalcante et al., 2004; Dondi et al., 2005). On the other hand, interparticle (open) porosity can influence the resistance to staining considering leaching and permeation of inhomogeneity from sources below the installed tiles and also from inside the ceramic body. The objectives of the present work were to investigate causes of color inhomogeneity in ceramic tiles, through the preparation of test specimens from the clays used as raw-materials by the local ceramic industry. Properties related to the sintering process such as the apparent density, water absorption, linear shrinkage, flexural strength and microstructure were also characterized and the conditions of defect formation were also simulated.

2. Experimental section

Prior to preparation of tile test specimens, the clays C1 and C2 have been dried at 110 °C for 24 h, dry-ground for 15 min in a ball mill, sifted through a 0.297 mm sieve and afterwards humidified at 6% water content.

2.1. Preparation of specimens

Test specimens were prepared by the pressing technique at a pressure of 19,6 MPa using (15×15×7) cm molds and then dried at 110 °C for 24 h. The specimens were fired in an electric Lavoisier 460 D furnace with a 7 °C/min heating rate at temperatures of 1000, 1120 and 1140 °C for 60 min, followed by natural cooling to room temperature. To simulate the conditions of formation of color inhomogeneities, the tile specimens have been chemically treated by immersion in 100 mL muriatic acid without dilution for 8 days at room temperature.

The densification behavior was studied by linear shrinkage (ABNT, 1984), water absorption (ASTM, 2000), apparent density, and flexural strength (ASTM, 1997). Linear shrinkage values upon drying and firing were evaluated from the variation of the length of the rectangular specimens. Water absorption values were determined from weight differences between the as-fired and water saturated samples (immersed in boiling water for 2 h). Apparent density was determined by the Archimedes method. The flexural strength was measured by the three point bending test.

2.2. Characterization techniques

Chemical composition of clays have been characterized by ICP-AES using an ARL 3410 instrument. Thermal analysis

(TGA) measurements were carried out using a TA SDT 2960 instrument, using Pt holders under N₂ flow of 100 mL/min and at a heating rate of 10 °C/min. X-ray diffractometry measurements for powdered samples were performed using Cu-Kα ($\lambda = 1.54060$ Å) on a Rigaku instrument, with 40 mA, 40 kV, and scanning rate of 3°/min. Scanning Electron Microscopy images were obtained with a JEOL JSM 6360LV microscope, in fracture mode for samples covered with a gold layer.

3. Results and discussion

Both clays presented high SiO₂, Al₂O₃ and Fe₂O₃ contents, reaching up to 70% to C1 and 87% for C2 (Table 1). The main differences between the two clays were the high CaO content of C1 and a lower SiO₂ percent. These differences suggest that the higher amount of gases formed in the firing step can give rise to a higher porosity in the tile specimens prepared from C1, which is also suggested by the higher thermal loss.

The X-ray diffractograms of the raw clays and after firing at 1000, 1120 and 1140 °C are presented in Fig. 1. C1 showed XRD reflections of illite ($2\theta = 9^\circ, 18^\circ$ and 20°) and kaolinite ($2\theta = 6.3^\circ, 12.5^\circ$ and 25°), in addition to calcite ($2\theta = 23^\circ, 29.4^\circ$ and 36°), feldspar ($2\theta = 27.5^\circ$) and quartz ($2\theta = 20.8^\circ, 26.6^\circ, 36.5^\circ, 39^\circ, 50^\circ$, and 60°) as main crystalline phases (JCPDS, 1995). After calcination the intensity of reflections at $2\theta = 9^\circ$ and $2\theta = 12.5^\circ$ (illite and kaolinite) decrease as a result of the formation of amorphous metakaolinite. The reflections at $2\theta = 22^\circ, 27.9^\circ, 30^\circ$ and 35.7° , increased in intensity indicating the formation of anorthite CaAl₂Si₂O₈, which is consistent with the higher calcium content in these specimens (Garcia et al., 1990), in addition to gehlenite Ca₂Al₂SiO₇ with reflections at $2\theta = 24^\circ, 29.2^\circ$, and 31.4° (Monteiro and Vieira, 2004). For C2, the X-ray diffractogram indicates illite, kaolinite, quartz and feldspar. Upon heating reflections from illite, kaolinite and feldspar decreased and finally disappeared, leaving quartz as the main crystalline component.

Table 1
Chemical composition of the clays (mass %)

Composition	C1	C2
SiO ₂	50.1	66.0
Al ₂ O ₃	15.0	16.4
Fe ₂ O ₃	5.5	4.1
K ₂ O	2.8	3.6
MgO	2.5	1.8
Na ₂ O	0.8	1.1
TiO ₂	0.7	0.6
CaO	10.0	0.5
P ₂ O ₅	0.2	0.1
Loss of ignition	12.4	5.8

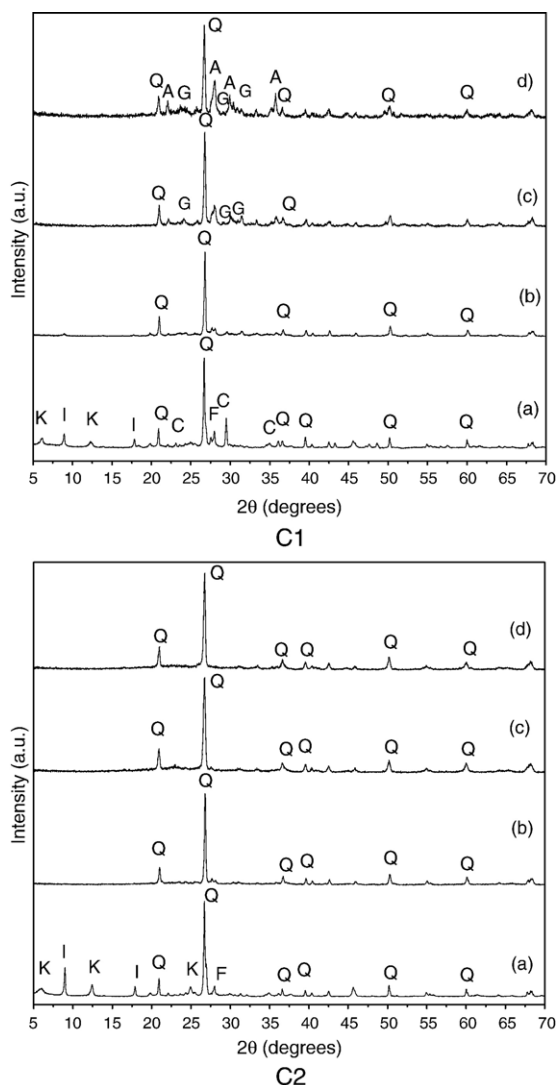


Fig. 1. Powder X-ray diffractograms of C1 and C2 clays (a) and calcined at 1000 (b), 1120 (c) and 1140 °C (d). Peaks in the diffractograms are identified as: Q: quartz; K: kaolinite; I: illite; A: anorthite, F: feldspar, and G: gehlenite.

Both clays eliminated adsorbed water around 100 °C, followed by dehydroxylation and elimination of organic matter up to 400 °C. For C1 the mass loss at 691 °C is due to carbonate decomposition. The presence of a high amount of CaCO_3 in C1 should explain the high weight loss and important porosity of the resulted product due to the CO_2 gas liberated which is harmful for the densification phenomenon (Fig. 2).

The densification behavior, in terms of apparent density as a function of temperature of ceramic specimens can be seen in Fig. 3. Only specimens prepared from C1 presented color inhomogeneity in the form of

large yellow stains. An increasing densification occurred above 1000 °C for both C1 and C2 specimens. However, the lower density values observed for specimens prepared from C1 (1.8–2.7 g/cm³) compared to C2 (2.6–3.5 g/cm³) are correlated to the higher porosity. The presence of CaCO_3 retards the sintering process since it modifies the formation of liquid phase responsible for the process (Escardino, 1993).

In most cases sintering contributes to enhancement of the flexural strength since decreasing porosity also reduces crack formation (Monteiro and Vieira, 2004). For both clays the flexural strength increases at increasing firing temperature (Fig. 4) as a result of sintering. The flexural strength values observed for C1 specimens were higher than those observed for C2 tiles, in spite of the observed density trends. This apparently contradictory observation can be understood by the formation of anorthite $\text{CaAl}_2\text{Si}_2\text{O}_8$ for C1 specimens at all temperatures studied, as evidenced by the XRD results, since anorthite has a high mechanical strength (Khalil and El-korashi, 1989). Thus the presence of anorthite compensates the higher porosity. Generally, raw materials for ceramic pastes containing CaCO_3 and

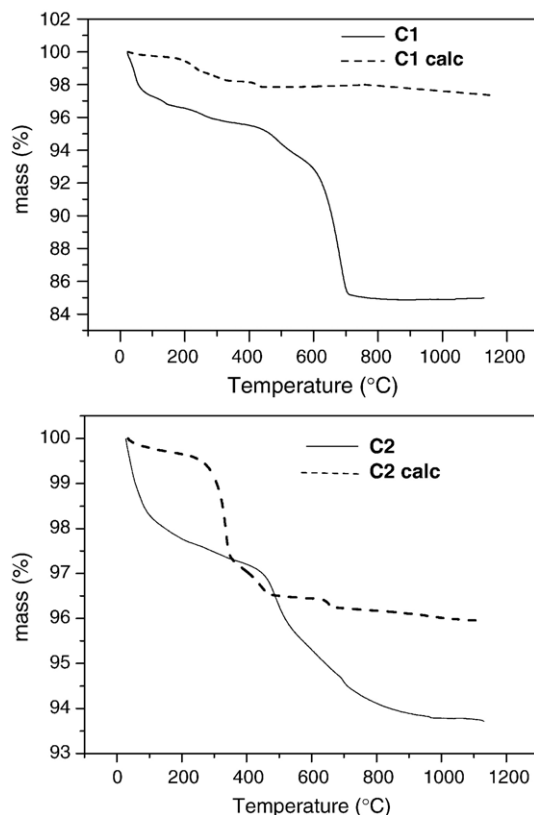


Fig. 2. TGA curves of C1 and C2 and after calcination at 1120 °C (C1 calc and C2 calc).

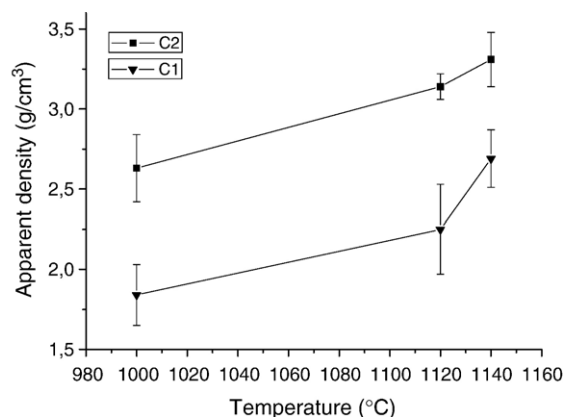


Fig. 3. Apparent density versus firing temperature for ceramic specimens prepared from C1 and C2.

alumina silicates are prompt to form crystalline phases at relatively low temperatures (from 950 °C–1000 °C). As a consequence, even with high porosity, the resulted products present good strength. The pores here are generally intergranular compared to closed porosity concentrated in the amorphous regions of vitrified (due to the liquid) ceramic (Kamseu et al., 2007).

Temperature-dependence curves for water absorption (WA) and linear shrinkage (LS) of ceramic materials are known as gresification diagrams, in which LS maximum coincide with WA minimum at the optimum firing temperature (Monteiro and Vieira, 2004). Gresification diagrams represent the microstructural evolution during the firing process due to the dependence of both parameters on sintering as well as porosity (Lieberman and Schulle, 1999). According to technical standards, tiles with water absorption values higher than 10% are classified as porous wall tiles. The gresification

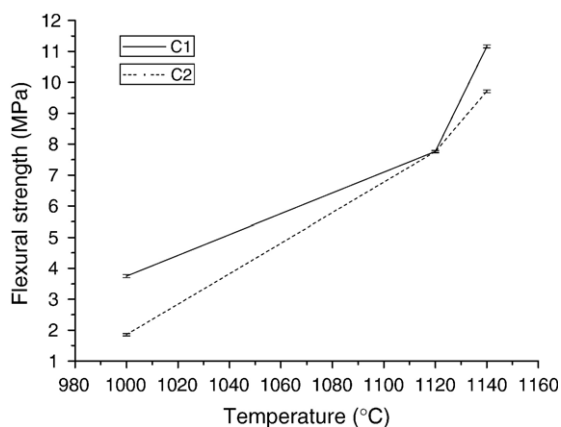


Fig. 4. Flexural strength of tile specimens from C1 and C2.

diagrams, Fig. 5, indicate that the tile specimens prepared from C2 presented significant variations both in the water absorption and linear shrinkage values, evidencing the occurrence of vitrification and densification. On the other hand, tile specimens from C1 did not present significant variations of the parameters measured, indicating that the water absorption remained relatively high in addition to small degrees of linear shrinkage at the temperature range studied. This behavior indicates that optimum fire temperatures for this composition probably lies above the range studied, as also observed by Sousa and co-workers (Sousa and Holanda, 2005) for CaCO_3 contents ranging from 12 to 18%. During heating below 900 °C CaCO_3 decomposes to CaO which reacts with metakaolinite. The series of reactions with the formation of small volumes of liquid phase, as expected, resulted in a body with high open porosity. Also, the linear shrinkage and water absorption of the sintered bodies varied only slightly in the temperature range studied. Thus, the ceramic tiles prepared from C1 have been fired at temperatures below

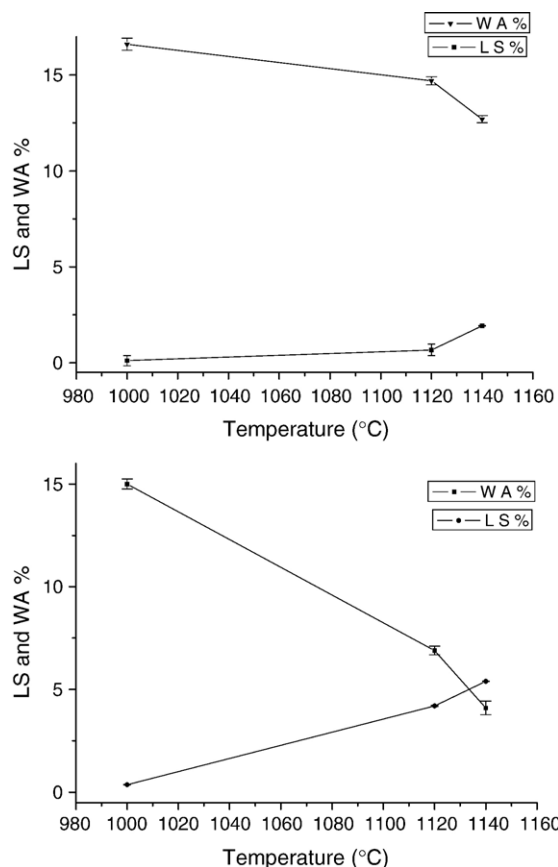


Fig. 5. Linear shrinking (LS) and water absorption (WA) for tiles prepared from C1 and C2.

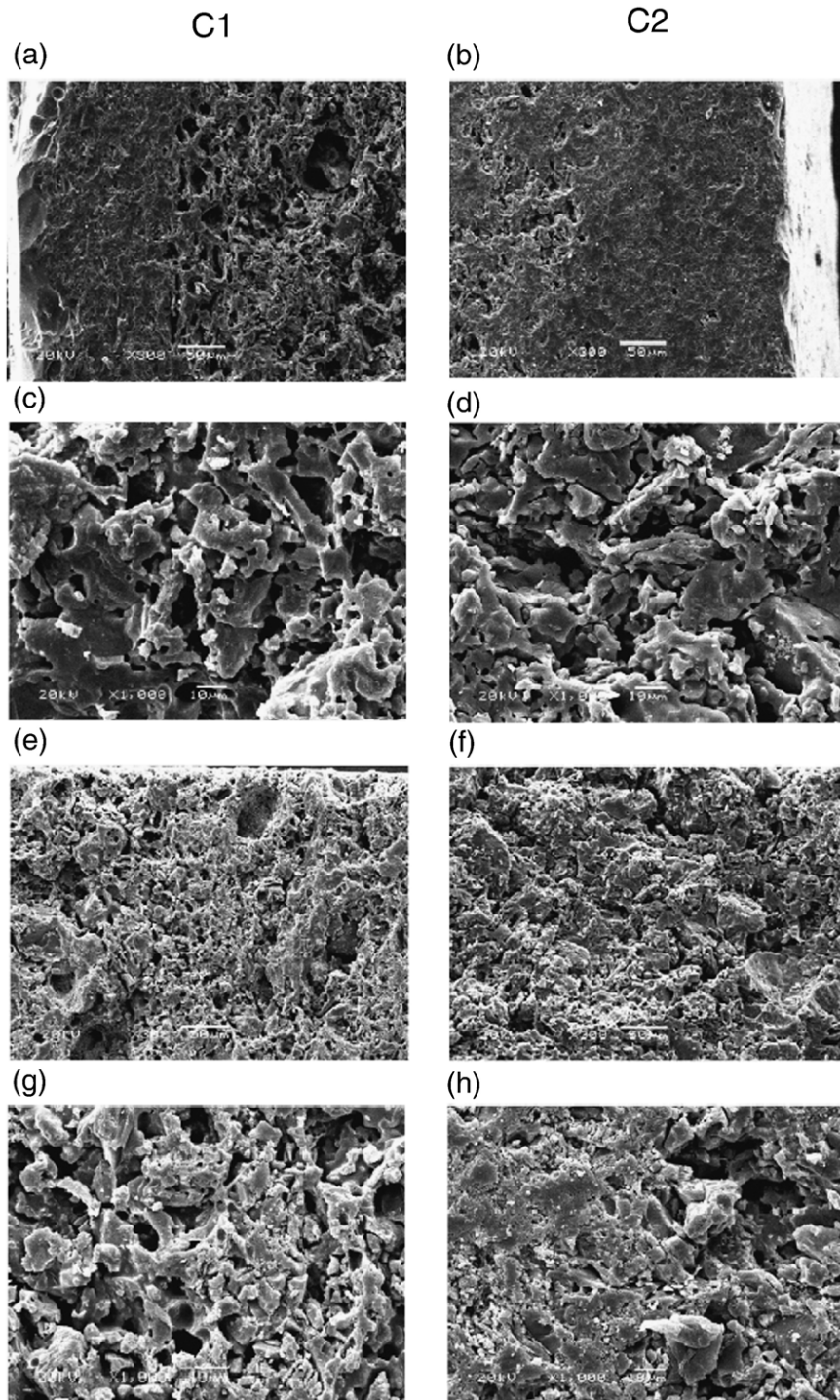


Fig. 6. SEM images of tiles prepared from C1 and C2 fired at 1120 °C (a, c, e, g) and 1140 °C (b, d, f, h).

the optimal sintering range, which probably contributed to the high porosity and consequently to stain formation.

The examination of microstructure by SEM, Fig. 6, confirmed that C1 ceramic tiles presented a higher

porosity than the specimens based on C2. The presence of open pores in the form of intraparticle voids, Fig. 6a, and also of sponge-like pores, Fig. 6b–c, are observed at several magnifications, showing the lower sintering

degree of bodies from C1. The sponge-like pores probably were formed by CaCO_3 decomposition and the intraparticle voids were progressively removed by sintering, observed by comparison of images from C1 (Fig. 6a, c, e, g) and C2 (Fig. 6b, d, f, h).

4. Conclusions

During heating up to 1140 °C, the higher CaCO_3 content of C1 retarded the sintering process, causing a higher porosity of C1 tiles. As a consequence, C1 tiles presented relatively high water absorption and low linear shrinkage, along with low staining resistance. Due to the presence of anorthite, the flexural strength of C1 specimens was higher than those of C2 specimens.

Acknowledgements

The authors are grateful to SAMARSA, FAPITEC, IEL/SEBRAE/CNPq-BITEC and to LQES-IQ/UNICAMP.

References

- ABNT, NBR MB 305, 1984. Determinação da Retração Linear.
- Arantes, F.J.S., Galesi, D.F., Quinteiro, E., Boschi, A.O., 2001. O manchamento e a porosidade fechada de gres porcelanato. *Ceram. Ind.* 6, 18–25.
- ASTM, 1997. C 674-77. Flexural Properties of Ceramic Whiteware Materials.
- ASTM, 2000. C 20-00. Test Method for Water Absorption, Bulk Density, Apparent Porosity and Apparent Specific Gravity of Fired Whiteware Products.
- Cavalcante, P.M.T., Dondi, M., Ercolani, G., Guarini, G., Melandri, C., Raimondo, M., Almendra, E.R., 2004. The influence of microstructure on the performance of white porcelain stoneware. *Ceram. Int.* 30, 953–959.
- Dondi, M., Ercolani, G., Guarini, G., Melandri, C., Raimondo, M., Rocha, Almendra E., Cavalcante, P.M.T., 2005. The role of surface microstructure on the resistance to stains of porcelain stoneware tiles. *J. Eur. Ceram. Soc.* 25, 357–365.
- Escardino, A., 1993. Single-fired ceramic wall tile manufacture. *Tile Brick Int.* 9, 14–19.
- Garcia, F.G., Acosta, V.R., Ramos, G.G., Rodriguez, M.G., 1990. Firing transformations of mixtures of clays containing illite, kaolinite and calcium carbonate used by ornamental tile industries. *Appl. Clay Sci.* 5, 361–375.
- JCPDS, 1995. ICDD.
- Kamseu, E., Leonelli, C., Boccaccini, D.N., Veronesi, P., Miselli, P., Pellacani, M.G.U.C., 2007. Characterisation of porcelain compositions using two china clays from Cameroon. *Ceram. Int.* 33, 851–857.
- Khalil, A.A.A., El-korashy, S.A., 1989. Firing characteristics of Sinai calcareous clays. *Ceram. Int.* 15, 297–303.
- Lieberman, H., Schulle, W., 1999. Basic properties of clay mineral raw materials and their influence on the microstructural formation during sintering. *Ceram. Forum Int.* 76, 31–34.
- Monteiro, S.N., Vieira, C.M.F., 2004. Influence of firing temperature on the ceramic properties of clays from Campos dos Goytacases, Brazil. *Appl. Clay Sci.* 27, 229–234.
- Sanchez, E., Ibanez, M.J., Garcia-Tena, J., Quereda, M.F., Hutchings, I.M., Xu, Y.M., 2006. Porcelain tile microstructure: Implications for polished tile properties. *J. Eur. Ceram. Soc.* 26, 2533–2540.
- Sánchez-Muñoz, L., Cava, S.S., Paskocimas, C.A., Cerisuelo, E., Longo, E., Carda, J.B., 2002a. Influence of raw materials composition on the vitrification process of ceramic tiles. *Ceramica* 48, 137–145.
- Sánchez-Muñoz, L., Cava, S.S., Paskocimas, C.A., Cerisuelo, E., Longo, E., Carda, J.B., 2002b. Modelling of the vitrification process of ceramic bodies for whiteware. *Ceramica* 43, 217–222.
- Sousa, S.J.G., Holanda, J.N.F., 2005. Development of red wall tiles by the dry process using Brazilian raw materials. *Ceram. Int.* 31, 215–222.